

Experimental Study of the Thermal Conductivity of Single-Walled Carbon Nanotube-Based Thin Films

I. A. Tambasov^{a,*}, A. S. Voronin^b, N. P. Evsevskaya^c, Yu. M. Kuznetsov^d, A. V. Luk'yanyenko^{a,e},
E. V. Tambasova^f, M. O. Gornakov^a, M. V. Dorokhin^d, and Yu. Yu. Loginov^f

^a Kirensky Institute of Physics, Krasnoyarsk Science Centre of the Siberian Branch of Russian Academy of Science, Krasnoyarsk, 660036 Russia

^b Krasnoyarsk Science Centre of the Siberian Branch of Russian Academy of Science, Krasnoyarsk, 660036 Russia

^c Institute of Chemistry and Chemical Technology, Krasnoyarsk Science Centre of the Siberian Branch of Russian Academy of Science, Krasnoyarsk, 660036 Russia

^d Nizhny Novgorod State University, Research Institute of Physics and Technology, Nizhny Novgorod, 603950 Russia

^e Siberian Federal University, Krasnoyarsk, 660041 Russia

^f Siberian State University of Science and Technology, Krasnoyarsk, 660014 Russia

*e-mail: tambasov_igor@mail.ru

Received November 11, 2019; revised January 21, 2020; accepted January 21, 2020

Abstract—The single-walled carbon nanotube-based thin films with a thickness from 11 ± 3 to 157 ± 18 nm have been formed using vacuum filtration. The thermal conductivity of the thin films as a function of thickness and temperature up to 450 K has been studied by the 3ω technique. It has been found that, in the region of 49 nm, the supplied heat from a gold strip started propagating with the high efficiency to the thin film plane. The thermal conductivity of the thin films with a thickness of 49 ± 8 nm was measured using the 3ω technique for bulk samples. It has been found that the thermal conductivity of the single-walled carbon nanotube-based thin films strongly depends on their thickness and temperature. The thermal conductivity sharply (by a factor of ~ 60) increases with an increase in thickness from 11 ± 3 to 65 ± 4 nm. In addition, it has been observed that the thermal conductivity of the thin film with a thickness of 157 ± 18 nm rapidly decreases from 211 ± 11 to 27.5 ± 1.4 W m⁻¹ K⁻¹ at 300 and 450 K, respectively.

Keywords: single-walled carbon nanotubes, vacuum filtration, thin films, thermal conductivity

DOI: 10.1134/S1063783420060311

1. INTRODUCTION

Different allotropic forms of carbon are the key materials for flexible electronics [1, 2]. In terms of the development and creation of prototypes of flexible electronic devices, single-walled carbon nanotubes (SWCNTs) are promising [1, 3]. To design flexible electronic devices, including flexible thermoelectric converters [4], on the basis of SWCNTs, the heat transfer mechanism should be known. Heat transfer in the SWCNT-based systems is fairly complex and depends on the formed structure of a system. The mechanism of heat transfer in single- and multi-walled carbon nanotubes has a phonon nature [5]. When the mean phonon free path is longer than a nanotube, the phonon transport is ballistic [6]. The main dissipation channel is phonon–phonon scattering by the crystal lattice defects. In most applied problems, just the SWCNT-based thin films are used [1–3, 7]. A new effective scattering channel provided by the

contacts between nanotubes is formed in the films. As was shown in reviews [8, 9], the thermal conductivity of the carbon nanotube-based structures can change from 0.1 to 6600 W m⁻¹ K⁻¹. Thus, the experimental study of the thermal conductivity of the SWCNT-based film systems as a function of the film thickness and geometric parameters (length and diameter) of individual nanotubes is a key task.

In this study, we report for the first time the measurements of the thermal conductivity of the thin films based on commercial SWCNTs using the 3ω technique. A strong dependence of the thermal conductivity on the thickness and temperature was established.

2. TECHNIQUES FOR THE FILM SYNTHESIS AND STUDY

Aqueous dispersions were prepared from a Tuball dry raw SWCNT powder (OCSiAl) and the sodium

cholate surfactant (2 wt % in the aqueous dispersion). According to previous studies [3, 10], these SWCNTs have a diameter in the range of about 1.6–1.9 nm. The SWCNT-based thin films were obtained by vacuum filtration. The technique for preparing the dispersions and SWCNT-based thin films was described in detail in [10]. The substrate used was AGC display glass. The thickness of the SWCNT films was determined by transmission electron microscopy on a Hitachi TM7700 electron microscope in the cross-sectional mode [10, 11]. It should be noted here that the carbon nanotube-based thin films had a nonuniform thickness [10]. To analyze the film thickness, ten measurements of the cross-sectional image for each sample were performed. The thickness of a thin film was determined as the arithmetic mean of ten measurements with the standard deviation. Thus, in this work, we studied the SWCNT films with thicknesses of 11 ± 3 , 34 ± 12 , 49 ± 8 , 65 ± 4 , and 157 ± 18 nm, respectively. The surface morphology of the thin films was determined on a Nanoink DPN 5000 atomic force microscope.

To measure the thermal conductivity of the SWCNT thin films, the 3ω technique was used. For this purpose, gold strips were formed by optical photolithography on each SWCNT film. Each gold strip had a length of 3 mm, a width of 20 μm , and a thickness of 40 nm. To provide electrical insulation, an Al_2O_3 dielectric layer was formed between a thin SWCNT film and a gold strip. The Al_2O_3 -layer thickness was ~ 7 nm. This Al_2O_3 thickness ensured the electrical insulation and introduced a minimum error in the thermal conductivity of the measured thin film. The gold and Al_2O_3 layers on a glass substrate and thin SWCNT films were obtained by electron beam deposition in a single process. Hereinafter, it is meant that, when measuring the frequency dependence of the substrate, the 7-nm Al_2O_3 layer/glass substrate system is, in fact, measured.

Using a Keithley 6221 meter, we specified an ac current flowing through the gold strip, according to the 3ω technique. The amplitude of the generated third harmonic was measured with a Stanford Research System SR810 selective voltmeter. The thermal conductivity in the SWCNT thin films was measured in the temperature range of 300–450 K. All the measurements were performed in vacuum under a residual pressure below 3 Pa.

The study of the thermal conductivity of thin films has certain features. Using the 3ω technique, we measured $U_{3\omega}$ as a function of $\text{Ln}(2\omega)$ of the substrate, where $U_{3\omega}$ is the amplitude of the voltage generated at a tripled frequency and ω is the frequency of the ac current supplied to the gold strip. Then, the measurements of $U_{3\omega}$ as a function of $\text{Ln}(2\omega)$ of the film/substrate system were performed. In the $U_{3\omega}(\text{Ln}(2\omega))$ dependences, the linear portion was found. After that, a linear approximation of these two dependences was

made. The difference between the constants of the film/substrate system and the substrate obtained by approximating the dependences of $U_{3\omega}$ on $\text{Ln}(2\omega)$ in the linear portion determines the thermal conductivity of a thin film. According to the 3ω technique [12], the thermal conductivity coefficient κ of a thin film is distinguished as the frequency-independent term

$$\Delta T_{\text{film}} = \frac{2U_{3\omega \text{ film/substrate}}}{I_{\omega \text{ film/substrate}} R_2 \alpha} - \frac{2U_{3\omega \text{ substrate}}}{I_{\omega \text{ substrate}} R_1 \alpha} = \frac{Pt}{(l\kappa 2b)}, \quad (1)$$

$$\kappa = \frac{Pt}{(\Delta T_{\text{film}}/2b)}, \quad (2)$$

where $U_{3\omega \text{ film/substrate}}$ is the voltage amplitude at the tripled frequency in the film/substrate system, $I_{\omega \text{ film/substrate}}$ is the current amplitude at the fundamental frequency in the film/substrate system, α is the temperature coefficient of the electrical resistance of the gold strip, R_1 and R_2 are the electrical resistances of the gold strips used to measure the substrate and film/substrate system, $U_{3\omega \text{ substrate}}$ is the voltage amplitude at the tripled frequency during the substrate measurements, $I_{\omega \text{ substrate}}$ is the amplitude of the current at the fundamental frequency during the substrate measurements, P is the power supplied to the gold strip, t is the thickness of the investigated film, κ_{film} is the thermal conductivity coefficient of the thin film, and l and b are the length and half-width of the gold strip, respectively. As a matter of fact, the thin film acts as an additional thermal resistance [12]. The main measurement condition is the same heating of the substrate and film/substrate system. For this purpose, appropriate currents at the fundamental harmonic are selected according to the resistances of the gold stripes and the α value. Thus, upon analogous heating, the $U_{3\omega}(\text{Ln}(2\omega))$ dependence for the film/substrate system will be parallel to the $U_{3\omega}(\text{Ln}(2\omega))$ dependence for the substrate.

If the heat flux from the gold strip propagates into the depth to a distance smaller than the film thickness, then the bulk samples are measured using the approach based on the 3ω technique [13]. In this case, the thermal conductivity of the film will be determined using the formula

$$\kappa = -\frac{I_{\omega \text{ film/substrate}}^3 R_2^2 \alpha \partial \text{Ln}(2\omega)}{4l\pi \partial U_{3\omega}}, \quad (3)$$

where $\partial \text{Ln}(2\omega)/\partial U_{3\omega}$ is the reciprocal angular coefficient of the linear portion of the $U_{3\omega}(\text{Ln}(2\omega))$ function. In addition, the angular coefficient is found using the linear approximation.

The 3ω technique measures the thermal conductivity of thin films sufficiently accurately. In our case, the relative measurement error was $\leq 5\%$. The main contribution to the measurement error is made by the error of determination of the temperature coefficient of the electrical resistance of the gold strip and the

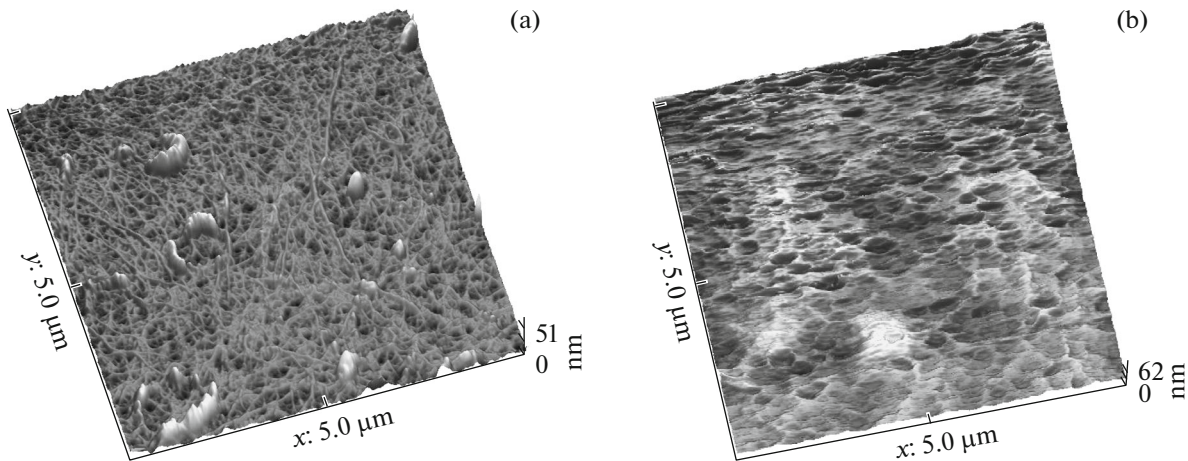


Fig. 1. Atomic force microscopy image of the SWCNT thin film with thicknesses of (a) 11 ± 3 and (b) 157 ± 18 nm.

slope of the experimental $U_{3\omega}(\text{Ln}(2\omega))$ dependence. The authors of [13–15] also mentioned that the relative error of the thermal conductivity measurements by the 3ω technique was no more than 2%.

3. EXPERIMENTAL RESULTS AND DISCUSSION

The surface of the SWCNT-based thin films with a thickness of 11 ± 3 and 157 ± 18 nm is shown in Figs. 1a and 1b, respectively.

On the surface of the SWCNT-based thin film with a thickness of 11 ± 3 nm, individual nanotubes can be distinguished. In addition, it can be seen that the surface is more porous than in the SWCNT-based thin film with a thickness of 157 ± 18 nm.

Figure 2 shows the $\Delta T(\text{Ln}(2\omega))$ dependence for five samples of the SWCNT thin films and a glass substrate.

It can be seen in Fig. 2 that only the $\Delta T(\text{Ln}(2\omega))$ dependences for the SWCNT thin films with thicknesses of 11 ± 3 and 34 ± 12 nm are parallel to the dependence for the substrate. This means that the heat flux from the gold strip passes through the SWCNT thin film into the substrate. In this case, the thermal conductivity coefficient was calculated using formula (2). An interesting effect is observed in the SWCNT film with a thickness of 49 ± 8 nm. Figure 2 shows that the $\Delta T(\text{Ln}(2\omega))$ dependence dramatically changes its slope relative to the dependence for the substrate. Physically, this situation can be explained by the fact that the heat flux efficiently spreads into the film plane. The investigated SWCNT thin film is a system of SWCNTs stacked in a plane. In experimental work [16], it was shown that the thermal conductivity of an individual SWCNT attains $3500 \text{ W m}^{-1} \text{ K}^{-1}$. Ultimately, a system of such nanotubes can distribute the heat flux into the film plane. However, a part of the

heat flux may reach the substrate. This case is the most complex for calculating the thermal conductivity of an SWCNT thin film, since the ratio between the heat flux transmitted to the substrate and the heat flux distributed in the plane is unknown. At thicknesses of 65 ± 4 and 157 ± 18 nm, the slopes of the $\Delta T(\text{Ln}(2\omega))$ dependences do not completely coincide with the dependence for the substrate. In this situation, the heat flux completely spreads into the plane of a SWCNT thin film and does not pass through the film/substrate interface. Thus, formula (2) was used to calculate the thermal conductivity of the SWCNT thin films with thicknesses of 11 ± 3 and 34 ± 12 nm and formula (3), for the films with thicknesses of 49 ± 8 , 65 ± 4 , and 157 ± 18 nm.

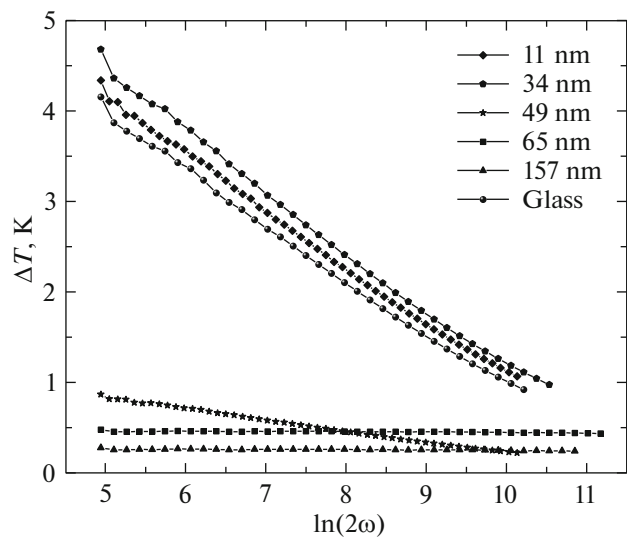


Fig. 2. Dependence of ΔT on $\text{Ln}(2\omega)$ for a glass substrate and SWCNT thin films with thicknesses of 11, 34, 49, 65, and 157 nm formed by vacuum filtration.

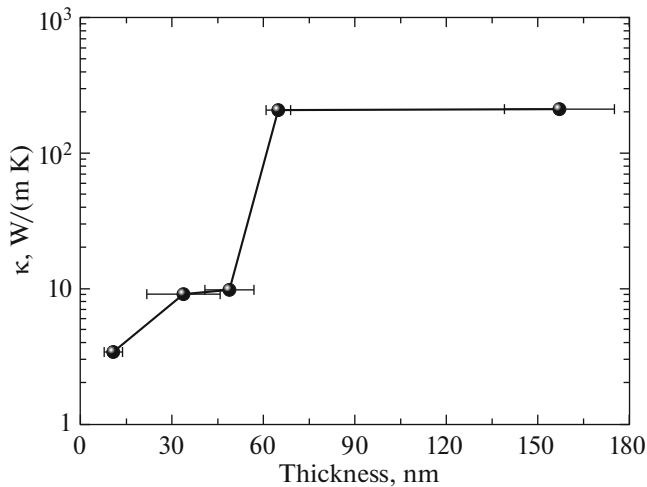


Fig. 3. Dependence of the thermal conductivity on the film thickness at room temperature.

Figure 3 shows the dependence of the thermal conductivity on the SWCNT thin film thickness.

It can be seen in Fig. 3 that the thermal conductivity strongly depends on the film thickness. At a film thickness of 11 ± 3 nm, the thermal conductivity coefficient was $3.42 \pm 0.17 \text{ W m}^{-1} \text{ K}^{-1}$. However, at a thickness of 65 ± 4 nm, the thermal conductivity coefficient attained $208 \pm 10 \text{ W m}^{-1} \text{ K}^{-1}$. The ratio between the thermal conductivity coefficients of the films with thicknesses of 65 ± 4 and 11 ± 3 nm was ~ 60 . A further increase in the film thickness almost does not affect the thermal conductivity. In particular, for the film with a thickness of 157 ± 18 nm, the thermal conductivity was $211 \pm 11 \text{ W m}^{-1} \text{ K}^{-1}$. We only found few works [17, 18] in which it was shown that the thermal conductivity depends on the film thickness. In these works, it was found that the thermal conductivity increases with the film thickness. However, we failed to find such a strong thickness dependence of the thermal conductivity in the literature. Possibly, at small thicknesses, the SWCNT thin films are formed with larger pores as compared with the thick films. This likely leads to a decrease in the thermal conductivity. It is worth noting here that, for the thin film with a thickness of 49 ± 8 nm, the thermal conductivity is underestimated, since a part of the heat flux reaches the substrate. The calculation was made using formula (3) for bulk samples. Nevertheless, it was first found that the critical thickness of the SWCNT thin films at which the heat flux efficiently spreads into the film plane and is independent of the substrate is 49 ± 8 nm.

The temperature dependence of the thermal conductivity is shown in Fig. 4.

It can be seen in Fig. 4 that the thermal conductivity coefficient for the films with thicknesses of 11 ± 3 and 34 ± 12 nm depends relatively weakly on tempera-

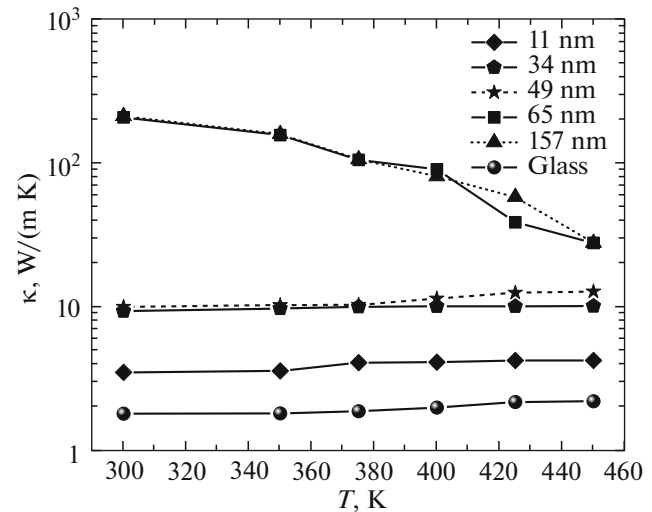


Fig. 4. Temperature dependence of the thermal conductivity for the SWCNT thin films with thicknesses of 11, 34, 49, 65, and 157 nm.

ture. Starting with a thickness of 49 ± 8 nm, the thermal conductivity increases from 375 K. At a temperature of 450 K, the thermal conductivity was $12.6 \pm 0.6 \text{ W m}^{-1} \text{ K}^{-1}$. A strong temperature effect was observed at thicknesses of 65 ± 4 and 157 ± 18 nm. With an increase in temperature, the thermal conductivity started sharply decreasing from $211 \pm 11 \text{ W m}^{-1} \text{ K}^{-1}$ at 300 K to $27.5 \pm 1.4 \text{ W m}^{-1} \text{ K}^{-1}$ at 450 K. The change by a factor of ~ 8 was observed. It should be noted that a value of $211 \pm 11 \text{ W m}^{-1} \text{ K}^{-1}$ at 300 K agrees well with the thermal conductivity for the 5- μm -thick SWCNT film [19]. In the literature, we found a few studies in which the thermal conductivity of the SWCNT thin films was measured above room temperature [20, 21]. In general, a similar temperature dependence of the thermal conductivity of the SWCNT thin films can be mentioned. However, such a strong temperature effect as in the films with thicknesses of 65 ± 4 and 157 ± 18 nm was not detected. A possible explanation of such a temperature dependence of the thermal conductivity can be the strong phonon scattering at the interface between nanotubes [20].

The thickness and temperature dependences of the thermal conductivity obtained in this work can be used to develop flexible electronics and SWCNT-based thermoelectric converters.

4. CONCLUSIONS

In this study, the SWCNT thin films with thicknesses of 11 ± 3 , 34 ± 12 , 49 ± 8 , 65 ± 4 , and 157 ± 18 nm were formed using vacuum filtration. To measure the thermal conductivity of the SWCNT thin films, the 3ω technique was used. The temperature measurements of the thermal conductivity were per-

formed in the temperature range of 300–450 K. For the first time, a transition thickness of 49 nm for the SWCNT thin films was determined, at which the thermal conductivity coefficient was measured with disregard of the substrate. A strong thickness dependence of the thermal conductivity was established. The change in the thickness from 11 ± 3 to 65 ± 4 nm led to an increase in the thermal conductivity by a factor of about 60. A strong temperature effect was observed in the films with thicknesses of 65 ± 4 and 157 ± 18 nm. The thermal conductivity coefficient of the film with a thickness of 157 ± 18 nm rapidly decreased from $211 \pm 11 \text{ W m}^{-1} \text{ K}^{-1}$ at 300 K to $27.5 \pm 1.4 \text{ W m}^{-1} \text{ K}^{-1}$ at 450 K. The change by a factor of ~ 8 was observed. The obtained thickness and temperature dependences of the thermal conductivity can be used in the development of flexible electronics, including thermoelectric converters, based on SWCNTs.

FUNDING

This study was supported by the Russian Foundation for Basic Research, the Government of the Krasnoyarsk Territory, and the Krasnoyarsk Territorial Foundation for Support of Scientific and R&D Activity, project Study of the Thermal Conductivity and Structural Features in Nanostructured Oxide Thin Films Promising for Thermoelectric Applications no. 18-42-243010 and the Scholarships of the President of the Russian Federation (SP-2235.2019.1).

CONFLICT OF INTEREST

The authors declare that they have no conflicts of interest.

REFERENCES

1. S. Park, M. Vosguerichian, and Z. A. Bao, *Nanoscale* **5**, 1727 (2013).
2. T. Cheng, Y. Z. Zhang, W. Y. Lai, and W. Huang, *Adv. Mater.* **27**, 3349 (2015).
3. I. A. Tambasov, A. S. Voronin, N. P. Evsevskaya, M. N. Volochaev, Y. V. Fadeev, A. S. Krylov, A. S. Aleksandrovskii, A. V. Luk'yanenko, S. R. Abelyan, and E. V. Tambasova, *Phys. Solid State* **60**, 2649 (2018).
4. J. L. Blackburn, A. J. Ferguson, C. Cho, and J. C. Grunlan, *Adv. Mater.* **30**, 1704386 (2018).
5. A. V. Eletsii, *Phys. Usp.* **52**, 209 (2009).
6. E. Brown, L. Hao, J. C. Gallop, and J. C. Macfarlane, *Appl. Phys. Lett.* **87**, 023107 (2005).
7. A. Kamyshny and S. Magdassi, *Chem. Soc. Rev.* **48**, 1712 (2019).
8. B. Kumanek and D. Janas, *J. Mater. Sci.* **54**, 7397 (2019).
9. A. D. Avery, B. H. Zhou, J. Lee, E. S. Lee, E. M. Miller, R. Ihly, D. Wesenberg, K. S. Mistry, S. L. Guillot, B. L. Zink, Y. H. Kim, J. L. Blackburn, and A. J. Ferguson, *Nat. Energy* **1**, 16033 (2016).
10. I. A. Tambasov, A. S. Voronin, N. P. Evsevskaya, M. N. Volochaev, Y. V. Fadeev, M. M. Simunin, A. S. Aleksandrovskiy, T. E. Smolyarova, S. R. Abelian, E. V. Tambasova, M. O. Gornakov, V. A. Eremina, Y. M. Kuznetsov, M. V. Dorokhin, and E. D. Obratsova, *Phys. E (Amsterdam, Neth.)* **114**, 113619 (2019).
11. I. A. Tambasov, M. N. Volochaev, A. S. Voronin, N. P. Evsevskaya, A. N. Masyugin, A. S. Aleksandrovskii, T. E. Smolyarova, I. V. Nemtsev, S. A. Lyashchenko, G. N. Bondarenko, and E. V. Tambasova, *Phys. Solid State* **61**, 1904 (2019).
12. D. G. Cahill, M. Katiyar, and J. R. Abelson, *Phys. Rev. B* **50**, 6077 (1994).
13. D. G. Cahill, *Rev. Sci. Instrum.* **61**, 802 (1990).
14. F. Chen, J. Shulman, Y. Xue, C. W. Chu, and G. S. Nolas, *Rev. Sci. Instrum.* **75**, 4578 (2004).
15. D. W. Oh, A. Jain, J. K. Eaton, K. E. Goodson, and J. S. Lee, *Int. J. Heat Fluid Flow* **29**, 1456 (2008).
16. E. Pop, D. Mann, Q. Wang, K. E. Goodson, and H. J. Dai, *Nano Lett.* **6**, 96 (2006).
17. S. Yoshida, Y. Feng, C. Delacou, T. Inoue, R. Xiang, R. Kometani, S. Chiashi, E. I. Kauppinen, and S. Maruyama, *Nanotechnology* **28**, 185701 (2017).
18. Y. Feng, T. Inoue, M. Watanabe, S. Yoshida, Y. Qian, R. Xiang, E. I. Kauppinen, S. Chiashi, and S. Maruyama, *Jpn. J. Appl. Phys.* **57**, 075101 (2018).
19. J. Hone, M. C. Llaguno, N. M. Nemes, A. T. Johnson, J. E. Fischer, D. A. Walters, M. J. Casavant, J. Schmidt, and R. E. Smalley, *Appl. Phys. Lett.* **77**, 666 (2000).
20. A. Duzynska, A. Taube, K. P. Korona, J. Judek, and M. Zdrojek, *Appl. Phys. Lett.* **106**, 183108 (2015).
21. M. Yarali, J. Hao, M. Khodadadi, H. Brahmī, S. Chen, V. G. Hadjiev, Y. J. Jung, and A. Mavrokefalos, *RSC Adv.* **7**, 14078 (2017).

Translated by E. Bondareva